gle and double substitutions were created in each of these secondary structures, and the ability of FhaC variants to interact with FHA was assessed (fig. S6) by using an overlay assay developed previously (*25*). Modifications in H2 affected FHA recognition by FhaC in this overlay assay, indicating that helix H2 forms part of the specific recognition surface of FHA.

Collectively, previous data (*15*) and our new mutagenesis data indicate that the L6 loop–motif 3 and the POTRA domains, which are the hallmark features of the superfamily, constitute the active secretion elements of FhaC. FHA is a 50-nm elongated right-handed parallel β helix (*26*–*28*), with the adherence determinants presented on loops or extrahelical motifs along the β helix. The helix interior is essentially filled with stacks of aliphatic residues (Val, Leu, Ile, Ala, and Gly), a characteristic often observed in such β helices. In the light of our structural and functional analysis of FhaC, we propose the following model for transport of FHA across the outer membrane (Fig. 4). The N-terminal TPS domain of FHA, which is characteristic of TpsA proteins and harbors specific secretion signals, initially interacts in an extended conformation with the POTRA 1 domain in the periplasm. Given the orientation of the POTRA domains relative to the channel, the FHA-FhaC interactions bring the region corresponding to the first repeats of the central β-helical domain of FHA in proximity to the tip of loop L6. Conformational changes in FhaC would then expel loop L6 out of the β barrel, opening a 8 Å to 16 Å large (depending on whether H1 is inside or outside the channel during secretion) channel for FHA translocation (fig. S4, C and D). In either case, the channel would not be wide enough to support internal folding of the repeated β-helical motifs of FHA; thus, this event likely takes place at the cell surface. FHA may form a hairpin made up of two extended polypeptide chains in the channel, with its TPS domain anchored in the periplasm. The first repeats of the adhesin could then reach the cell surface, where they could progressively fold into β-helical coils. The formation of the FHA rigid β helix may provide the energy to drive its translocation through FhaC. Transport of FHA in this direction is in agreement with the observation that the C terminus of FHA is exposed to the cell surface before its N terminus (*29*). After the C terminus of FHA has reached the surface, the TPS domain could dissociate from the POTRA domains and be translocated, capping the N terminus of the FHA β helix. Lastly, loop L6 could move back into the barrel.

Because most TpsA proteins are predicted to fold into β helical structures (*26*, *27*), the transport mechanism proposed here may apply more generally to the secretion of TpsA proteins by their dedicated TpsB transporters. All members of the Omp85-TpsB superfamily harbor one to several POTRA domains followed by a β barrel, as well as conserved motifs corresponding to the L6 loop within the barrel, and they mostly handle substrate proteins rich in β structure. Therefore, the major features described here are likely to remain valid throughout the family, although more complex molecular events are expected for some of those transporters, given that they are part of macromolecular assemblies.

References and Notes

1. M.-R. Yen *et al.*, *Biochim. Biophys. Acta* **1562**, 6 (2002).
2. F. Jacob-Dubuisson, R. Fernandez, L. Coutte, *Biochim. Biophys. Acta* **1694**, 235 (2004).
3. S. C. Hinnah, K. Hill, R. Wagner, T. Schlicher, J. Soll, *EMBO J.* **16**, 7351 (1997).
4. B. Bolter, J. Soll, A. Schulz, S. Hinnah, R. Wagner, *Proc. Natl. Acad. Sci. U.S.A.* **95**, 15831 (1998).
5. V. Kozjak *et al.*, *J. Biol. Chem.* **278**, 48520 (2003).
6. S. A. Paschen *et al.*, *Nature* **426**, 862 (2003).
7. R. Voulhoux, M. P. Bos, J. Geursten, M. Mols, J. Tommassen, *Science* **299**, 262 (2003).
8. I. Gentle, K. Gabriel, P. Beech, R. Waller, T. Lithgow, *J. Cell Biol.* **164**, 19 (2004).
9. T. Wu *et al.*, *Cell* **121**, 235 (2005).
10. I. E. Gentle, L. Burri, T. Lithgow, *Mol. Microbiol.* **58**, 1216 (2005).
11. L. Sanchez-Pulido, D. Devos, S. Genevrois, M. Vicente, A. Valencia, *Trends Biochem. Sci.* **28**, 523 (2003).
12. R. Voulhoux, J. Tommassen, *Res. Microbiol.* **155**, 129 (2004).
13. S. Moslavac *et al.*, *FEBS J.* **272**, 1367 (2005).
14. Materials and methods are available as supporting material on *Science* Online.
15. S. Guédin *et al.*, *J. Biol. Chem.* **275**, 30202 (2000).
16. A. C. Méli *et al.*, *J. Biol. Chem.* **281**, 158 (2006).
17. P. Van Gelder, F. Dumas, M. Winterhalter, *Biophys. Chem.* **85**, 153 (2000).
18. The POTRA domains superimpose with an RMS displacement of 1.6 Å, calculated for the Cα. Well-conserved secondary structures include helices H2 and H4, strands β2 and β5, and strands β3 and β6 from POTRA 1 and POTRA 2, respectively.
19. Single-letter abbreviations for the amino acid residues are as follows: A, Ala; C, Cys; D, Asp; E, Glu; F, Phe; G, Gly; H, His; I, Ile; K, Lys; L, Leu; M, Met; N, Asn; P, Pro; Q, Gln; R, Arg; S, Ser; T, Thr; V, Val; W, Trp; and Y, Tyr.
20. C. J. Oomen *et al.*, *EMBO J.* **23**, 1257 (2004).
21. Planar lipid bilayer experiments on the translocator domain of NalP revealed openings and closings of pores of two sizes, with single-channel conductances of 0.15 nS and 1.3 nS that correspond to pore dimensions of 2.4 Å and 8.4 Å, respectively (*20*). Displacement of the α helix from the pore would result in an open channel that may correspond to the observed 1.3-nS conductance steps in planar lipid bilayer experiments. Furthermore, deletion of the α helix in NalP was also shown to increase pore activity (*20*). This helix must be outside the channel to allow for secretion of the passenger domain and could subsequently move in to plug the pore.
22. K. L. Lou *et al.*, *J. Biol. Chem.* **271**, 20669 (1996).
23. N. Saint *et al.*, *J. Biol. Chem.* **271**, 20676 (1996).
24. P. S. Phale *et al.*, *Proc. Natl. Acad. Sci. U.S.A.* **94**, 6741 (1997).
25. H. Hodak *et al.*, *Mol. Microbiol.* **61**, 368 (2006).
26. A. V. Kajava *et al.*, *Mol. Microbiol.* **42**, 279 (2001).
27. B. Clantin *et al.*, *Proc. Natl. Acad. Sci. U.S.A.* **101**, 6194 (2004).
28. FHA comprises an N-terminal TPS domain folded into a β helix, with three extrahelical motifs, a β hairpin, a four-stranded β sheet, and an N-terminal capping (*27*). The reported structure of a 30-kD N-terminal fragment of FHA (Fha30) also reveals several β-helical repeats that form the central right-handed β helix domain of the full-length adhesin.
29. J. Mazar, P. A. Cotter, *Mol. Microbiol.* **62**, 641 (2006).
30. W. L. DeLano, PyMOL Molecular Graphics System (2002); www.pymol.org.

31. We thank H. Hodak for the gift of Fha30 and FhaC-N^{myc} and for advice with the overlay assay experiments, E. Willery and M. L. Parsy for the antibiotic susceptibility experiments, H. Belrhali for support at beamline BM14 at the European Synchrotron Radiation Facility (ESRF, Grenoble), and H. Drobecq for expert assistance with the mass spectrometry experiments. A.C.M. and P.R. are the recipients of predoctoral fellowships from the French Minister de l'Education Nationale and Recherche and Technologie. B.C., F.J.-D., and V.V. are researchers of the CNRS. This work was supported in part by an ACI BCMS2004 grant from the French Ministry of Research. V.V. is supported by an Action Thématique et Incitative sur Programme program from the CNRS and by the Region Nord-Pas de Calais through the Contrat de Plan État-Région and Fonds Européen de Développement Régional programs. Coordinates and structure factors have been deposited in the Protein Data Bank with accession code 2QDZ.

Supporting Online Material

www.sciencemag.org/cgi/content/full/317/5840/957/DC1
Materials and Methods
Figs. S1 to S6
Tables S1 and S2
References

16 April 2007; accepted 11 July 2007
10.1126/science.1143860

Structure and Function of an Essential Component of the Outer Membrane Protein Assembly Machine

Seokhee Kim,[1] Juliana C. Malinverni,[2] Piotr Sliz,[3,4] Thomas J. Silhavy,[2] Stephen C. Harrison,[3,4] Daniel Kahne[1,3]*

Integral β-barrel proteins are found in the outer membranes of mitochondria, chloroplasts, and Gram-negative bacteria. The machine that assembles these proteins contains an integral membrane protein, called YaeT in *Escherichia coli*, which has one or more polypeptide transport–associated (POTRA) domains. The crystal structure of a periplasmic fragment of YaeT reveals the POTRA domain fold and suggests a model for how POTRA domains can bind different peptide sequences, as required for a machine that handles numerous β-barrel protein precursors. Analysis of POTRA domain deletions shows which are essential and provides a view of the spatial organization of this assembly machine.

Although most biological membranes contain exclusively α-helical proteins, the outer membrane of Gram-negative bacteria and the organellar membranes of mitochondria and chloroplasts contain β-barrel proteins (*1*). These integral β-barrel proteins, called outer membrane proteins (OMPs), are folded and inserted into membranes by a process, conserved between prokaryotes and eukaryotes (*2*–*4*), that involves the action of a multiprotein

machine (*5*, *6*). Genetic and biochemical experiments have identified many parts of this machine in several organisms, including *Saccharomyces cerevisiae* and *E. coli* (*3*–*13*). The only conserved component in prokaryotes and eukaryotes is an integral β-barrel membrane protein, represented by YaeT in *E. coli*, Sam50 in mitochondria, and a Toc75 isoform in chloroplasts. A substantial region of all three proteins projects into the intermembrane space and contains one or more predicted polypeptide transport–associated (POTRA) domains (*3*, *4*, *14*).

Proteins destined for the outer membrane of *E. coli* are synthesized in the cytoplasm and transported across the inner membrane through the SecYEG protein secretion machinery (Fig. 1) (*15*). The signal sequence targeting them for secretion is removed at the outer face of the inner membrane. The processed OMP then traverses the periplasmic compartment to β-barrel assembly sites in the outer membrane. Chaperones may assist in periplasmic passage (*16*). It is presumed that the processed OMPs contain structural features that allow them to be recognized by the β-barrel assembly machinery, which in *E. coli* consists of at least five interacting components: four lipoproteins (YfgL, YfiO, NlpB, and SmpA) and the conserved integral membrane protein, YaeT (*5*, *13*).

There are homologs of YaeT in organisms from bacteria to humans (*17*). Recent experiments with *E. coli* YaeT and *S. cerevisiae* Sam50 have shown that these proteins are essential for viability. Furthermore, levels of folded β-barrel proteins decrease and levels of misfolded β-barrel proteins increase when they are depleted (*4*, *5*, *7*, *8*, *18*, *19*). YaeT was reported to bind C-terminal peptides of OMPs (*20*). The POTRA domain in Sam50 was shown to bind unfolded β-barrel precursors, suggesting that this POTRA domain plays an important role in assembling other β-barrel proteins in the mitochondrial membrane (*21*). Biochemical studies of truncated variants of Toc75 have also implicated its POTRA domains as docking sites for proteins destined to be targeted to, or across, biological membranes (*22*). No structure of a POTRA domain has yet been reported.

We expressed and purified the periplasmic domain of *E. coli* YaeT containing all five POTRA domains ($YaeT_{21\text{-}420}$) (*23*, *24*). Crystallization of this construct was unsuccessful, but a shorter fragment containing four POTRA domains (residues 21 to 351) yielded well-ordered crystals with diffraction to spacings of 2.2 Å (*23*, *24*).

The overall structure of $YaeT_{21\text{-}351}$ has a fishhook-like shape, with successive POTRA domains rotated in a right-handed direction (Fig. 2, A and B). Despite having low sequence similarity, the POTRA domains have similar

[1]Department of Chemistry and Chemical Biology, Harvard University, Cambridge, MA 02138, USA. [2]Department of Molecular Biology, Princeton University, Princeton, NJ 08544, USA. [3]Department of Biological Chemistry and Molecular Pharmacology, Harvard Medical School, Boston, MA 02115, USA. [4]Howard Hughes Medical Institute and Children's Hospital Laboratory of Molecular Medicine, Boston, MA 02115, USA.

*To whom correspondence should be addressed. E-mail: kahne@chemistry.harvard.edu

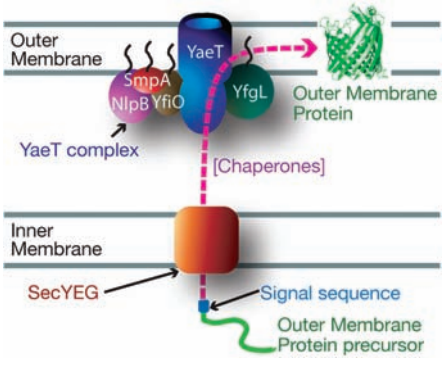

Fig. 1. Diagram of bacterial outer membrane protein (OMP) biogenesis.

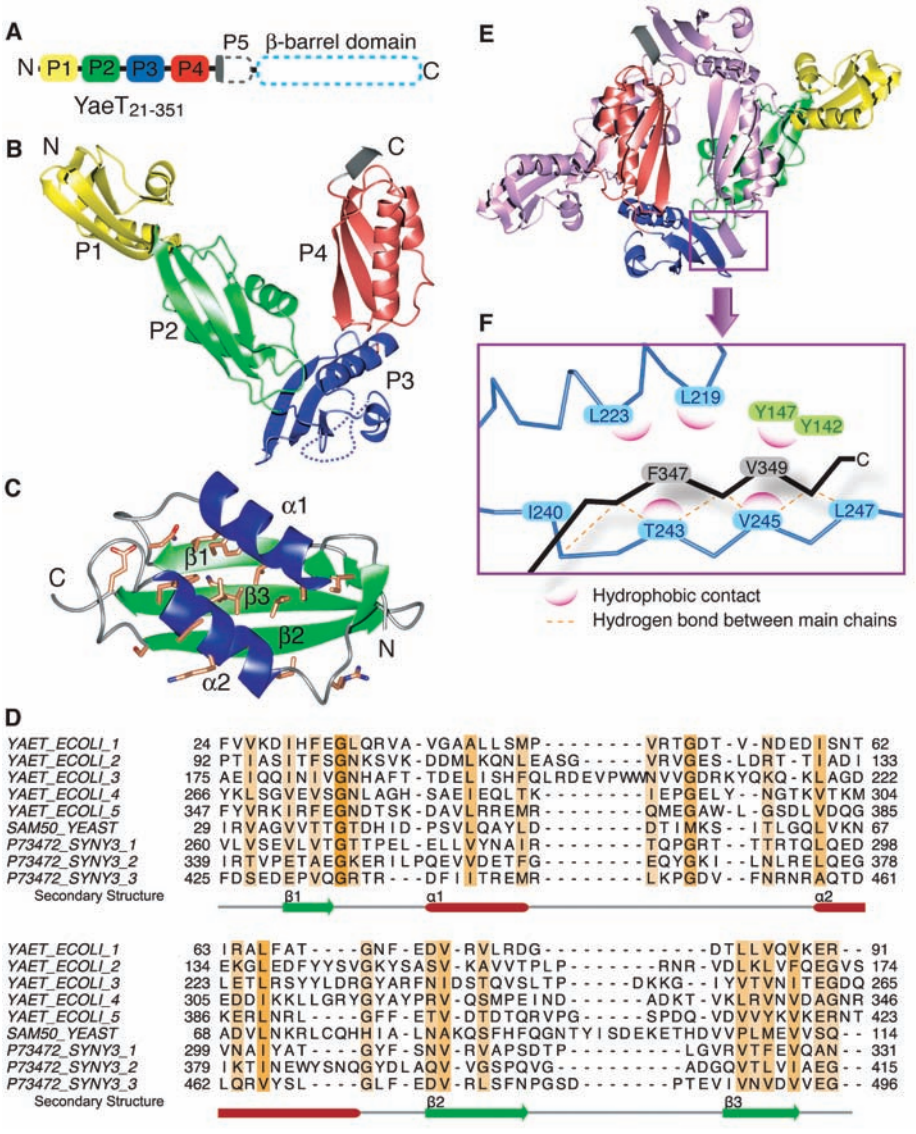

Fig. 2. Structure of YaeT. (**A**) Domain organization. (**B**) X-ray structure of $YaeT_{21\text{-}351}$. POTRA domains P1 to P4 are colored yellow, green, blue, and red, respectively. The eight residues from P5 are colored gray. The missing electron density in the P3 domain is represented by a dashed line. (**C**) Ribbon diagram of a POTRA domain (P2) with side chains of the conserved residues shown. (**D**) Sequence alignments of POTRA domains from selected members of the YaeT/Omp85, Sam50, and Toc75 families, found in Gram-negative bacteria, mitochondria, and chloroplasts or cyanobacteria, respectively [adapted from Sánchez-Pulido *et al.* (*14*)]. Conserved residues are highlighted (*28*). The intensity of the orange color reflects the level of conservation in physicochemical properties. (**E**) X-ray structure of the dimer. The POTRA domains in one monomer are colored as in (B); the other monomer is purple. (**F**) Dimer interface showing the C-terminal residue contacts of one monomer (gray) to the P2 (light green) and P3 (light blue) domains of the other monomer. Labels represent hydrophobic residues. L, Leu; Y, Tyr; F, Phe; V, Val; I, Ile; T, Thr.

folds, comprising a three-stranded β sheet overlaid with a pair of antiparallel helices (Fig. 2C). The order of secondary-structure elements is β-α-α-β-β (disproving a previous prediction (*14*); the first and second β strands form the two edges of the sheet, with the β3 strand sandwiched between them. The conserved residues that define the POTRA domains are primarily in the hydrophobic core or loop regions, suggesting that they are important for the structural integrity of POTRA domain (Fig. 2, C and D).

$YaeT_{21\text{-}351}$ is a dimer in the crystal (Fig. 2E). The two monomers are intertwined, burying 1900 $Å^2$ of solvent-accessible surface of each monomer. The longest contiguous set of contacts between monomer units involves a series of main-chain hydrogen bonds between the β2 edge of the P3 domain of one monomer (Asp^{241} to Leu^{247}) and the first residues (Asn^{345} to Lys^{351}) of the truncated P5 domain of the other monomer (Fig. 2F). These residues form a parallel β strand with respect to the β2 edge of the P3 domain and bury ~1000 $Å^2$, more than half the total buried surface. There are no other extensive contacts between monomers, suggesting that dimerization is mediated by this parallel β-stranded interface. Formation of this interface may have been necessary for growth of well-ordered crystals given that slightly shorter ($YaeT_{21\text{-}348}$) or longer ($YaeT_{21\text{-}355}$) constructs failed to crystallize. Nonetheless, highly ordered contacts are conserved at the interfaces between successive POTRA domains (fig. S1), suggesting that the fishhook conformation is present in the monomer.

We do not think that the dimer is physiologically relevant for several reasons. First, $YaeT_{21\text{-}351}$ elutes as a monomer from a size exclusion column (fig. S2), implying that the stability of the dimer observed in the crystal is weak. Second, the N terminus of P5, which forms one of the β strands of the dimer interface, would not be available to interact with P3 in the full-length protein because the interacting residues

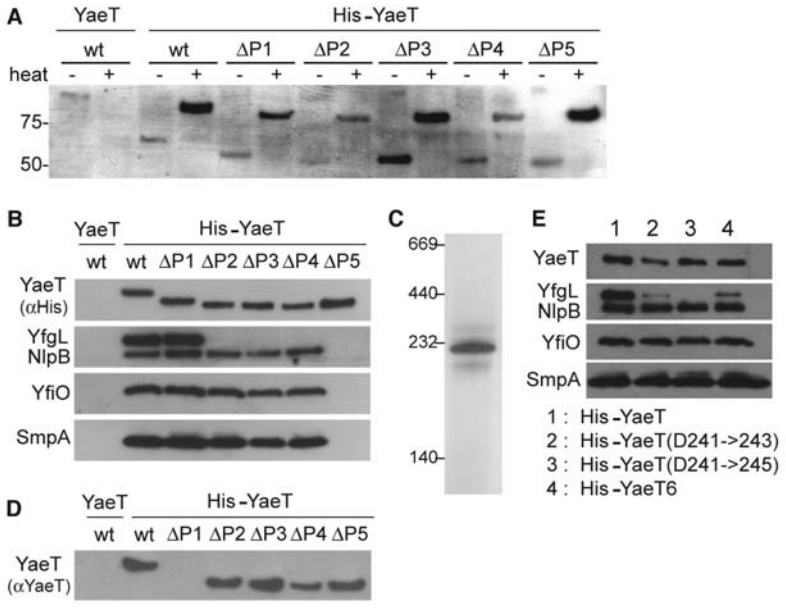

Fig. 3. (**A**) SDS-PAGE analysis of YaeT wild-type (wt) and deletion mutants from whole-cell lysates, without (–) and with (+) prior heat treatment. Proteins were detected by Western blot analysis with the use of an antibody recognizing the His tag. (**B**) His-tagged YaeT wild-type or deletion mutants (ΔP1 to ΔP5) and associated proteins following Ni-affinity chromatography. Eluted samples were blotted against His-tag, YfgL, NlpB, SmpA, and YfiO antibodies. (**C**) The purified YaeT complex run on a Blue-Native PAGE with molecular weights from a standard lane indicated. (**D**) Same as in (B), but YaeT was blotted with an antibody to YaeT. YaeTΔP1 cannot be detected with our YaeT peptide antibody. (**E**) His-tagged wild-type YaeT and P3 mutants after purification by Ni-affinity chromatography and analysis, as in (B).

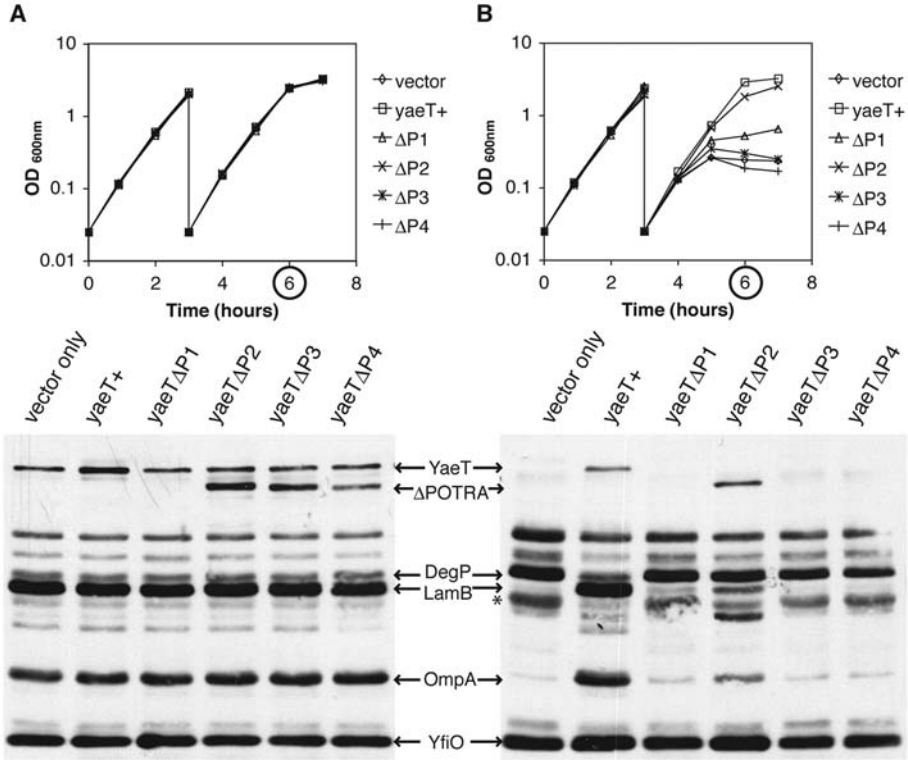

Fig. 4. Essentiality of POTRA domains. Cultures were grown with L-arabinose (A) or D-fucose (B) to induce or inhibit wild-type *yaeT* expression, which is driven by the ara P_{BAD} promoter (*5*). Plasmid-borne *yaeT* variants were constitutively expressed. Samples taken after 6 hours were subjected to Western analysis. (**A**) Strains expressing plasmid-borne *yaeT* variants grew normally when wild-type *yaeT* was expressed. YaeTΔP1 cannot be recognized with our YaeT peptide antibody (Fig. 3). Strains have low levels of DegP and normal OMP levels (LamB and OmpA). (**B**) When wild-type YaeT is absent, strains producing mutant YaeT variants exhibit growth defects. Strains expressing ΔP1 and ΔP2 grow better and have higher levels of OMPs than ΔP3, ΔP4, and the vector-only control. Although levels of ΔP1 cannot be quantified, ΔP2 is stable, indicating insertion into the membrane even in the absence of wild-type YaeT. Nevertheless, all strains lacking wild-type YaeT exhibit a strong extracytoplasmic stress response (increased DegP) indicative of OMP-assembly defects. Asterisk in (B) corresponds to proteolyzed DegP. OD, optical density.

would be buried in the P5 hydrophobic core. Nevertheless, the dimer interface shows that one way in which other polypeptides can interact with POTRA domains is by β augmentation (*25*).

The lipoproteins in the OMP assembly complex reside in the periplasmic space along with the five POTRA domains of YaeT. One function of the POTRA domains in YaeT could be to provide a scaffold to organize these lipoproteins. Using the crystal structure as a guide, we prepared five N-terminally His-tagged YaeT deletion constructs, each lacking a POTRA domain. All five deletion constructs (YaeTΔP1 to YaeTΔP5) could be expressed in an *E. coli* strain containing a wild-type chromosomal *yaeT* gene; all were targeted to the outer membrane and folded as judged by heat modifiability (Fig. 3A). Each deletion construct was purified by Ni-affinity chromatography, and eluents were assayed to determine which lipoproteins were present. Any of the first four POTRA domains can be deleted without disrupting the interactions with YfiO, NlpB or SmpA; however, the P5 deletion loses all three of these lipoproteins (Fig. 3B). YfgL disappears when any POTRA domains except P1 are deleted (Fig. 3B). These studies show that the periplasmic portion of YaeT scaffolds the other four proteins; and the studies also outline the spatial organization of the OMP assembly complex. Although YaeT purified from inclusion bodies is reported to form higher-order oligomers (*20*), the multiprotein OMP assembly complex behaves as a monomer. It has a mobility on Blue-Native polyacrylamide gel electrophoresis (PAGE) corresponding to a mass less than 230 kD (Fig. 3C). Furthermore, wild-type YaeT does not associate with the His-tagged YaeT POTRA domain deletion mutants (Fig. 3D).

To assess the functional importance of each POTRA domain, we constructed five POTRA domain deletion mutants without His tags for complementation studies in an *E. coli* YaeT-depletion strain. The ΔP1 and ΔP2 mutant proteins retained partial function: Strains expressing these proteins can survive YaeT depletion but grow poorly (Fig. 4). Strains producing the ΔP3 and ΔP4 mutant proteins did not survive YaeT depletion (Fig. 4), showing that P3 and P4 are essential for viability even though neither scaffolds an essential lipoprotein. The ΔP5 construct could not be introduced into the YaeT-depletion strain even under conditions where wild-type YaeT was expressed. Apparently, the ΔP5 mutant protein is toxic to cells in this context. Because we cannot detect an interaction between the mutant protein and wild-type YaeT or any of the lipoproteins, we suggest that ΔP5 mishandles nascent β-barrel substrates, producing harmful misfolded or aggregated OMPs.

P3 has a feature not present in the others—a β bulge (Ile^{240} and Asp^{241}) in strand β2. This strand is at the edge that binds the vestigial residues of P5, and the bulge appears to expose the strand for β augmentation. To determine whether this feature of P3 is involved in an essential function of YaeT or in its association with YfgL, we moved Asp^{241} two and four residues along the β strand to alter the likely location of the bulge and to reduce or disrupt the potential for β augmentation. These bulge translation mutants were expressed at wild-type levels. The two- and four-residue shifts decreased and abolished, respectively, binding to YfgL (Fig. 3E), but both mutants complemented the YaeT deletion strain. These results show that the edge of P3 participates in binding YfgL but that the essential functions of P3 do not involve the modified edge of the domain, nor do they require its interactions with YfgL, as expected from the nonessential nature of this lipoprotein.

The crystal structure may also hold clues to other functionally important regions of P3. The only residues in the polypeptide chain that are not resolved in the crystal structure are located within the loop between the α1 and α2 helices of P3. We have previously isolated a mutant that encodes a YaeT variant, YaeT6, which contains a two–amino acid insertion in the same region of the α1-α2 loop (*12*) of P3. YaeT6, which retains the ability to bind YfgL (Fig. 3E) as well as the other three proteins of the OMP assembly complex, compromises OMP assembly in a wild-type background, but suppresses the outer membrane permeability defects conferred by *imp4213*, a mutant allele of an essential gene that encodes an OMP that is required for lipopolysaccharide assembly (*26*). The α1-α2 loop of P3 may interact with Imp, providing an explanation for why mutations that alter the loop suppress the permeability defects caused by *imp4213*.

Notably, β-strand augmentation (*25*), observed in the dimer interface of the YaeT crystal structure, occurs in other complexes that bind unfolded OMPs—for example, the PDZ domain of DegS, which helps clear misfolded OMPs from the periplasm (*27*). We have shown that P3 may bind YfgL in this way, and it is possible that other POTRA domains, which also contain exposed edges, interact with polypeptides by β-strand augmentation. This mode of capture would allow POTRA domains to participate in assembling the β barrels of OMPs in a manner that is insensitive to the diversity of their primary sequences but dependent on their common hydrophobic periodicity.

References and Notes

1. W. C. Wimley, *Curr. Opin. Struct. Biol.* **13**, 404 (2003).
2. S. Reumann, J. Davila-Aponte, K. Keegstra, *Proc. Natl. Acad. Sci. U.S.A.* **96**, 784 (1999).
3. R. Voulhoux, M. P. Bos, J. Geurtsen, M. Mols, J. Tommassen, *Science* **299**, 262 (2003).
4. S. A. Paschen *et al.*, *Nature* **426**, 862 (2003).
5. T. Wu *et al.*, *Cell* **121**, 235 (2005).
6. N. Wiedemann *et al.*, *Nature* **424**, 565 (2003).
7. V. Kozjak *et al.*, *J. Biol. Chem.* **278**, 48520 (2003).
8. I. Gentle, K. Gabriel, P. Beech, R. Waller, T. Lithgow, *J. Cell Biol.* **164**, 19 (2004).
9. N. Pfanner, N. Wiedemann, C. Meisinger, T. Lithgrow, *Nat. Struct. Mol. Biol.* **11**, 1044 (2004).
10. S. A. Paschen, W. Neupert, D. Rapaport, *Trends Biochem. Sci.* **30**, 575 (2005).
11. N. Ruiz, B. Falcone, D. Kahne, T. J. Silhavy, *Cell* **121**, 307 (2005).
12. N. Ruiz, T. Wu, D. Kahne, T. J. Silhavy, *ACS Chem. Biol.* **1**, 385 (2006).
13. J. G. Sklar *et al.*, *Proc. Natl. Acad. Sci. U.S.A.* **104**, 6400 (2007).
14. L. Sánchez-Pulido, D. Devos, S. Genevrois, M. Vicente, A. Valencia, *Trends Biochem. Sci.* **28**, 523 (2003).
15. A. K. Veenendaal, C. van der Does, A. J. Driessen, *Biochim. Biophys. Acta* **1694**, 81 (2004).
16. J. E. Mogensen, D. E. Otzen, *Mol. Microbiol.* **57**, 326 (2005).
17. S. Moslavac *et al.*, *FEBS J.* **272**, 1367 (2005).
18. W. T. Doerrler, C. R. Raetz, *J. Biol. Chem.* **280**, 27679 (2005).
19. J. Werner, R. Misra, *Mol. Microbiol.* **57**, 1450 (2005).
20. V. Robert *et al.*, *PLoS Biol.* **4**, e377 (2006).
21. S. J. Habib *et al.*, *J. Cell Biol.* **176**, 77 (2007).
22. F. Ertel *et al.*, *J. Biol. Chem.* **280**, 28281 (2005).
23. Residues 1 to 20 represent the signal sequence.
24. Materials and methods are available as supporting material on *Science* Online.
25. S. C. Harrison, *Cell* **86**, 341 (1996).
26. M. P. Bos, B. Tefsen, J. Geurtsen, J. Tommassen, *Proc. Natl. Acad. Sci. U.S.A.* **101**, 9417 (2004).
27. C. Wilken, K. Kitzing, R. Kurzbauer, M. Ehrmann, T. Clausen, *Cell* **117**, 483 (2004).
28. M. Clamp, J. Cuff, S. M. Searle, G. J. Barton, *Bioinfomatics* **20**, 426 (2004).

29. This work is supported by NIH grants GM66174 (D.K.) and GM34821 (T.J.S.). S.C.H. is a Howard Hughes Medical Institute investigator. Data was collected at beamline ID19 at the Advanced Photon Source, Argonne National laboratory, which is supported by the U.S. Department of Energy, under contract no. W-31-109-ENG-38. We thank J. J. Miranda and R. Meijers for technical support. Coordinates and structure factors have been deposited in the Protein Data Bank with the accession codes 2QCZ and 2QDF.

Supporting Online Material

www.sciencemag.org/cgi/content/full/317/5840/961/DC1
Materials and Methods
Figs. S1 to S3
Tables S1 and S2
References

18 April 2007; accepted 3 July 2007
10.1126/science.1143993

Structure and Function of an Essential Component of the Outer Membrane Protein Assembly Machine

Seokhee Kim *et al.*

Science **317**, 961 (2007);
DOI: 10.1126/science.1143993